

A Comparative Analysis of Scale-invariant Phenomena in Repeating Fast Radio Bursts and Glitching Pulsars

CHONG-YU GAO^{1,2} AND JUN-JIE WEI^{1,2} 

¹*Purple Mountain Observatory, Chinese Academy of Sciences, Nanjing 210023, China*

²*School of Astronomy and Space Sciences, University of Science and Technology of China, Hefei 230026, China*

ABSTRACT

The recent discoveries of a remarkable glitch/antiglitch accompanied by fast radio burst (FRB)-like bursts from the Galactic magnetar SGR J1935+2154 have revealed the physical connection between the two. In this work, we study the statistical properties of radio bursts from the hyperactive repeating source FRB 20201124A and of glitches from the pulsar PSR B1737–30. For FRB 20201124A, we confirm that the probability density functions of fluctuations of energy, peak flux, duration, and waiting time well follow the Tsallis q -Gaussian distribution. The derived q values from q -Gaussian distribution keep approximately steady for different temporal interval scales, which indicate that there is a common scale-invariant structure in repeating FRBs. Similar scale-invariant property can be found in PSR B1737–30’s glitches, implying an underlying association between the origins of repeating FRBs and pulsar glitches. These statistical features can be well understood within the same physical framework of self-organized criticality systems.

Keywords: Radio transient sources (2008) — Radio bursts (1339) — Pulsars (1306)

1. INTRODUCTION

Fast radio bursts (FRBs) are intense millisecond-duration astronomical transients with mysterious physical origins (Lorimer et al. 2007; Xiao et al. 2021; Petroff et al. 2022; Zhang 2023). Some FRB sources, such as FRB 20121102 (Spitler et al. 2016) and FRB 20201124A (Lanman et al. 2022), have been seen to burst repeatedly, but it is still unclear whether repeating FRBs are prevalent or rare sources. Nonetheless, the statistical analysis of the repetition pattern may shed new light on the physical nature and emission mechanisms of FRBs (e.g., CHIME/FRB Collaboration et al. 2020a; Rajwade et al. 2020; Zhang 2020; Cruces et al. 2021; Li et al. 2021b).

By studying the statistical properties of the repeating bursts from FRB 20121102, Lin & Sang (2020) and Wei et al. (2021) found that the probability density functions (PDFs) of fluctuations of energy, peak flux, and duration well follow a q -Gaussian distribution. Here the fluctuations are defined as the size (energy, peak flux, or duration) differences at different times. Furthermore, such a q -Gaussian behavior does not depend on the time interval adopted for the fluctuation, i.e., the q values in q -Gaussian distributions are approximately

equal for different temporal interval scales, which implies that there is a scale-invariant structure in FRB 20121102 (Lin & Sang 2020; Wei et al. 2021). Analogous scale-invariant characteristics have also been found in earthquakes (Caruso et al. 2007; Wang et al. 2015), soft gamma-ray repeaters (SGRs; Chang et al. 2017; Wei et al. 2021; Sang & Lin 2022), X-ray flares (Wei 2023) and precursors (Li & Yang 2023) of gamma-ray bursts (GRBs), and gamma-ray flares of the Sun and the blazar 3C 454.3 (Peng et al. 2023). It is suggested that scale invariance is the most essential hallmark of a self-organized criticality (SOC) system (Caruso et al. 2007; Wang et al. 2015). A generalized definition of SOC is that a non-linear dissipative system with external drives input will self-organize to a critical state, at which a small local disturbance would generate an avalanche-like chain reaction of any size within the system (Bak et al. 1987). Since the concept of SOC was proposed (Katz 1986; Bak et al. 1987), it has been extensively used to explain the dynamical behaviors of astrophysical phenomena (Aschwanden 2011, 2012, 2014, 2015; Aschwanden et al. 2016).

On 2020 April 28, a bright radio burst FRB 20200428 was independently detected by CHIME (CHIME/FRB Collaboration et al. 2020b) and STARE2 (Bochenek et al. 2020) in association with a hard X-ray burst from a Galactic magnetar named SGR J1935+2154 (Mereghetti et al. 2020; Li et al. 2021a; Ridnaia et al. 2021; Tavani et al. 2021). This discovery provided the first evidence for the magnetar ori-

gin of at least some FRBs (Zhang 2020). Since this event, *NICER* and *XMM-Newton* telescopes have been monitoring SGR J1935+2154 regularly in the 1–3 keV band. A phase-coherent timing analysis of X-ray pulses from the source was employed and a large spin-down glitch (also referred to as “antiglitch”) with $\Delta\nu = 1.8_{-0.5}^{+0.7} \mu\text{Hz}$ was detected on 2020 October 5 (± 1 day) (Younes et al. 2023). Subsequently, three FRB-like radio bursts emitted from SGR J1935+2154 were detected by the CHIME/FRB system on 2020 October 8 (Good & Chime/Frb Collaboration 2020). More surprisingly, Ge et al. (2022) utilized the observations from *NICER*, *NuSTAR*, *Chandra*, and *XMM-Newton* to study the timing properties of SGR J1935+2154 around the epoch of FRB 20200428, and reported that a giant spin-up glitch with $\Delta\nu = 19.8 \pm 1.4 \mu\text{Hz}$ occurred approximately 3.1 ± 2.5 day before FRB 20200428.

Glitches have now been observed in over a hundred pulsars, which are characterized as sudden increases in the rotational frequency of the star. Despite several decades of research, the physical mechanisms of glitches are still not completely understood, but probably involve an interaction between the neutron star’s outer elastic crust and the superfluid component that lies within (see Haskell & Melatos 2015; Antonopoulou et al. 2022 for reviews). The spin-down events, known as antiglitches, are even rarer than glitches, and lack of observational data. The exact origin of antiglitches is also still open to debate (Thompson et al. 2000; Huang & Geng 2014; Mastrano et al. 2015). The temporal coincidences between the glitch/antiglitch and FRB-like bursts of SGR J1935+2154 reveal the physical connection between the two (Ge et al. 2022; Wu et al. 2023; Younes et al. 2023). Motivated by this, we here examine the scale-invariant similarities between repeating FRBs and glitching pulsars.

Since the sample size of most repeaters in the past was small, FRB 20121102 with relatively more repeating bursts is so far the only source that has been used to study the scale-invariant property (Lin & Sang 2020; Wei et al. 2021). As more hyperactive repeaters have been detected, it is interesting to find out whether other FRBs share the same scale-invariant property. One of the most hyperactive repeating sources to date is FRB 20201124A, with 2744 independent bursts detected by the Five-hundred-meter Aperture Spherical radio Telescope (FAST), representing the largest sample for a single observation (Xu et al. 2022; Zhang et al. 2022). In addition, Kirsten et al. (2024) reported the detection of 46 high-energy bursts¹ from FRB 20201124A in more than 2000 hours using four small 25–32-m class radio telescopes. The

energy distribution slope of these high-energy bursts is much flatter than that of the high-energy tail in the FAST data, suggesting that ultra-high-energy ($E > 3 \times 10^{39}$ erg) bursts occur at a much higher rate than expected based on FAST observations of lower-energy bursts (Kirsten et al. 2024). The study on the scale-invariant properties of low- and high-energy bursts would be helpful for judging whether the highest-energy bursts originate from a different emission mechanism or emission region at the progenitor source. On the other hand, for glitching pulsars, their scale-invariant property has not yet been explored. However, because glitches are infrequent events, the number of detected glitches in most of pulsars is not substantial enough to carry out robust statistical analyses on individual bases (Fuentes et al. 2019). To date, 37 glitches in PSR B1737–30 have been detected, and these glitches exhibit a power-law size distribution. It should be underlined that the SOC systems would be slowly driven toward a critical state of the instability threshold of the entire system, leading to scale-free power-law size distributions (Aschwanden 2014). Thus, the emergence of a power-law size distribution is another fundamental property that SOC systems have in common (Aschwanden 2011, 2012, 2015), suggesting that PSR B1737–30 has enough glitches for studying its scale-invariant feature.

In this work, we investigate and examine the similar scale-invariant phenomena between FRB 20201124A and glitches of PSR B1737–30. Moreover, in view of the fact that the burst energy distribution of FRB 20201124A flattens towards the highest-observed energies, the sensitivity limits of FAST and 25–32-m class radio telescopes are different, and the statistical characteristics of 46 high-energy bursts would be submerged in the large amount of FAST data for the combined analysis, the scale-invariant behaviors of low- and high-energy bursts from FRB 20201124A are thus studied separately. The rest parts of this article are organized as follows. In Section 2, we make the scale-invariant analyses on energy, peak flux (luminosity), duration, and waiting time of low- and high-energy bursts from FRB 20201124A, respectively. In Section 3, taking PSR B1737–30 as an example, the distributions of fluctuations of glitch size and of waiting time between consecutive glitches are presented for the first time. Finally, relevant conclusions are drawn in Section 4.

2. SCALE INVARIANCE IN FRB 20201124A

2.1. Statistical properties of the FAST data

Recently, Xu et al. (2022) and Zhang et al. (2022) reported in total 2744 bursts from the repeating source FRB 20201124A detected by FAST from April 1 to June 11 and September 25 to October 17 in 2021. These observations were performed in the frequency range 1.0–1.5 GHz by using the center beam of the 19-beam receiver. Xu et al. (2022) detected 1863 bursts in 82 hours over 54 days, and Zhang et al.

¹ Note that in this paper, “high-energy burst” refers to bursts with large values of their isotropic energies, rather than bursts detected at higher observing frequencies.

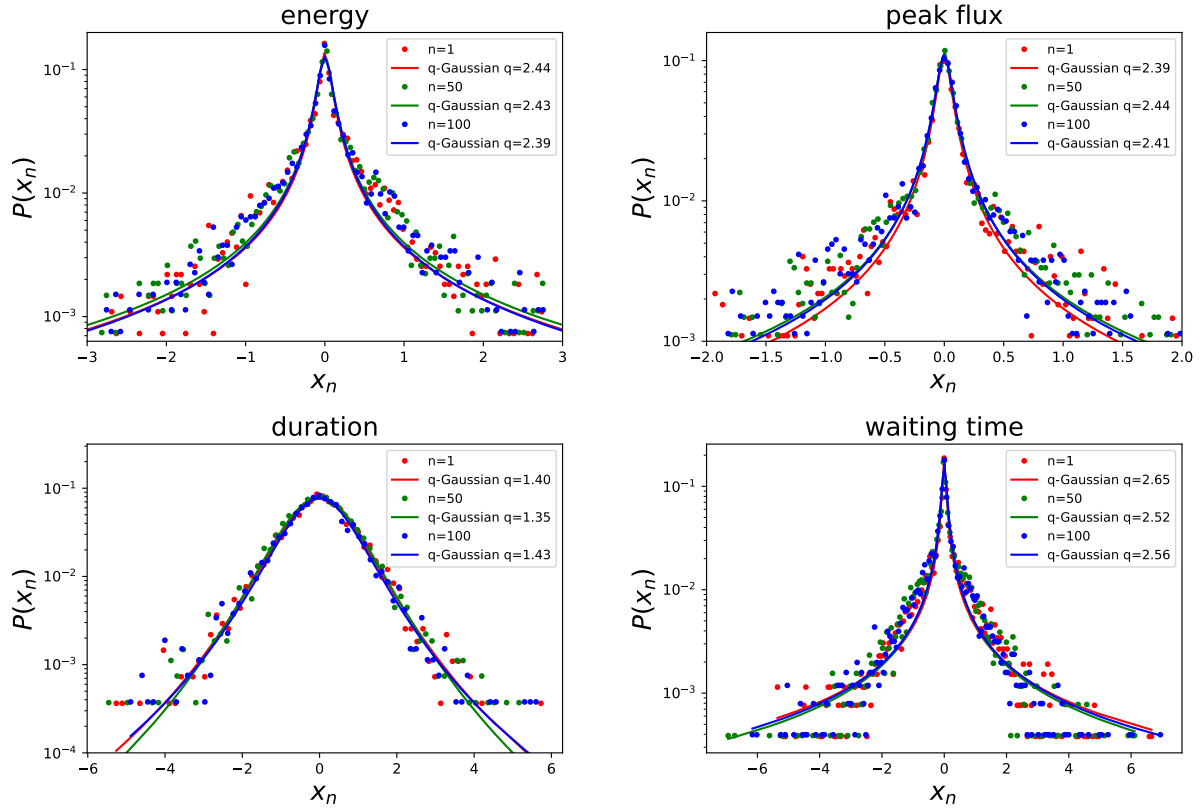


Figure 1. Statistical results of FRB 20201124A for the FAST sample. *Upper-left panel:* The PDFs of energy fluctuations $X_n = S_{i+n} - S_i$ for different temporal interval scales $n = 1$ (red dots), $n = 50$ (green dots), and $n = 100$ (blue dots). X_n is rescaled by the standard deviation of X_n , i.e. $x_n = X_n / \sigma_{X_n}$. The data are fitted by the q -Gaussian function (solid curves). *The other three panels:* The same data process and the fitting to the q -Gaussian function, except now for the PDFs of fluctuations of peak flux (upper-right panel), duration (lower-left panel), and waiting time (lower-right panel).

(2022) detected 881 bursts in 4 hours over 4 days. All these data were recorded with a frequency resolution of 122.07 kHz (i.e., using 4096 frequency channels to cover 1.0–1.5 GHz) and a time resolution of 49.152 μ s (Xu et al. 2022; Zhang et al. 2022; Zhou et al. 2022). The total of 2744 bursts from FRB 20201124A is at present the largest sample observed with a single instrument and uniform selection effects. In this work, we use this sample to study the PDFs of fluctuations of energy, peak flux, duration, and waiting time. FRB 20201124A was localized in a massive star-forming galaxy with a spectroscopic redshift of $z = 0.0979$ (Fong et al. 2021; Piro et al. 2021; Ravi et al. 2022; Xu et al. 2022). The known redshift allows us to infer the isotropic energy of each burst through $E = 4\pi D_L^2 F \Delta\nu / (1+z)$, where D_L is the luminosity distance, F is the burst fluence, and $\Delta\nu$ is the bandwidth. The waiting time is evaluated by the difference of times-of-arrival of two adjacent bursts.

The fluctuation of a size (e.g., energy, peak flux, duration, or waiting time) is defined as

$$X_n = S_{i+n} - S_i, \quad (1)$$

where S_i is the size of the i -th burst (or of the i -th pulsar glitch, more on this below) in temporal order, and n is an arbitrary integer denoting the temporal interval scale. In order to simplify the calculation, X_n is rescaled by

$$x_n = \frac{X_n}{\sigma_{X_n}}, \quad (2)$$

where σ_{X_n} is the standard deviation of X_n . We will analyze the statistical properties of the dimensionless fluctuations x_n .

Figure 1 shows the statistical results of FRB 20201124A for the FAST sample. We plot as colour dots the PDFs of fluctuations of energy (upper-left panel), peak flux (upper-right panel), duration (lower-left panel), and waiting time (lower-right panel) for the temporal interval scale $n = 1$ (red dots), $n = 50$ (green dots), and $n = 100$ (blue dots). Empirically, the data are binned with the Freedman-Diaconis rule (Freedman & Diaconis 1981). One can see from Figure 1 that compared to a Gaussian distribution, these PDFs $P(x_n)$ have a sharper peak at $x_n = 0$ and fatter tails. The sharp peak indicates that small fluctuations are most likely to occur, while fat tails indicate that there are large but rare fluctuations. Another remarkable feature is that the data points in Figure 1

Table 1. Fit results and estimated 68% confidence level constraints on the parameter q of the q -Gaussian function (Equation (3)) for different temporal interval scales n for repeating bursts of FRB 20201124A (including the samples of FAST and high-energy bursts) and glitches of PSR B1737–30

FRB 20201124A			
for the FAST sample			
parameters	$n = 1$	$n = 50$	$n = 100$
q -energy	$2.44^{+0.03}_{-0.03}$	$2.43^{+0.04}_{-0.04}$	$2.39^{+0.03}_{-0.03}$
χ^2_{red}	1.68	1.35	1.47
q -peak flux	$2.39^{+0.03}_{-0.03}$	$2.44^{+0.03}_{-0.03}$	$2.41^{+0.03}_{-0.03}$
χ^2_{red}	0.94	0.89	0.89
q -duration	$1.40^{+0.04}_{-0.04}$	$1.35^{+0.04}_{-0.04}$	$1.43^{+0.04}_{-0.04}$
χ^2_{red}	0.87	0.77	1.04
q -waiting time	$2.65^{+0.03}_{-0.03}$	$2.52^{+0.04}_{-0.04}$	$2.56^{+0.04}_{-0.03}$
χ^2_{red}	1.60	2.03	1.57
FRB 20201124A			
for the high-energy burst sample			
parameters	$n = 1$	$n = 5$	$n = 10$
q -energy	$2.29^{+0.13}_{-0.13}$	$2.41^{+0.13}_{-0.14}$	$2.51^{+0.13}_{-0.14}$
χ^2_{red}	0.05	0.13	0.13
q -luminosity	$2.27^{+0.13}_{-0.15}$	$2.40^{+0.13}_{-0.13}$	$2.40^{+0.15}_{-0.20}$
χ^2_{red}	0.11	0.05	0.08
q -duration	$2.05^{+0.15}_{-0.20}$	$2.19^{+0.14}_{-0.18}$	$1.95^{+0.23}_{-0.25}$
χ^2_{red}	0.09	0.09	0.15
q -waiting time	$1.95^{+0.16}_{-0.16}$	$2.07^{+0.20}_{-0.20}$	$2.23^{+0.28}_{-0.26}$
χ^2_{red}	0.18	0.11	0.13
PSR B1737–30			
parameters	$n = 1$	$n = 5$	$n = 10$
q -glitch size	$2.73^{+0.09}_{-0.11}$	$2.73^{+0.10}_{-0.14}$	$2.69^{+0.12}_{-0.15}$
χ^2_{red}	0.40	0.37	0.51
q -waiting time	$2.07^{+0.30}_{-0.33}$	$1.84^{+0.40}_{-0.31}$	$2.03^{+0.34}_{-0.43}$
χ^2_{red}	0.13	0.09	0.41

NOTE—The corresponding reduced chi-square χ^2_{red} are also listed in the table.

are almost independent of the interval n considered for the fluctuation, suggesting a common behavior of $P(x_n)$. Here we use the Tsallis q -Gaussian function (Tsallis 1988; Tsallis et al. 1998)

$$f(x_n) = \alpha [1 - \beta(1 - q)x_n^2]^{-\frac{1}{1-q}} \quad (3)$$

to fit $P(x_n)$, where α is a normalization factor, the parameters q and β determine the sharpness and width of the distribution, respectively. The q -Gaussian function is a generalization of the standard Gaussian function, and it reduces to a Gaussian shape with zero mean and standard deviation $\sigma = 1/\sqrt{2\beta}$ when q gets close to 1. Thus, $q \neq 1$ means a departure from Gaussian behavior.

For a specific n , the free parameters (α , β , and q) can be optimized by minimizing the χ^2 statistics,

$$\chi^2 = \sum_i \frac{[f(x_{n,i}) - P(x_{n,i})]^2}{\sigma_{P,i}^2}, \quad (4)$$

where $\sigma_{P,i} = \sqrt{N_{\text{bin},i}/N_{\text{tot}}}$ is the uncertainty of the data point, with $N_{\text{bin},i}$ being the number of x_n in the i -th bin and N_{tot} being the total number of x_n (Wei et al. 2021). Note that for the sake of clarity, the error bars of the data points are not plotted in the figure. We then adopt the Python Markov Chain Monte Carlo module, EMCEE (Foreman-Mackey et al. 2013), to perform the fitting. The red, green, and blue curves in Figure 1 stand for the best-fitting results for $n = 1$, $n = 50$, and $n = 100$, respectively. The best-fitting q values and their 1σ uncertainties for $n = 1, 50, 100$ are listed in Table 1, along with the reduced χ^2_{red} value for the fit. It is obvious that the PDFs of fluctuations of energy, peak flux, duration, and waiting time are well reproduced by means of q -Gaussians.

With the FAST data, we further extract the PDFs of fluctuations of energy, peak flux, duration, and waiting time for different scale intervals $1 \leq n \leq 100$, and fit the PDFs with the q -Gaussian function. The best-fitting q values as a function of n for energy, peak flux, duration, and waiting time are displayed in the left panel of Figure 2. One can see that the q values are approximately invariant and do not depend on the scale interval n , implying a scale-invariant structure of FRB 20201124A. The mean values of q for energy, peak flux, duration, and waiting time of the FAST data are 2.44 ± 0.03 , 2.40 ± 0.02 , 1.37 ± 0.03 , and 2.55 ± 0.03 , respectively, which are listed in Table 2. Here the uncertainties represent the 1σ standard deviations of q values. Interestingly, the q values we derived here are very close those of FRB 20121102 (Wei et al. 2021), which suggest that there is a common scale-invariant structure in repeating FRBs.

Xu et al. (2022) estimated the sample completeness for the FAST data, and showed that the fluence threshold achieving the 95% detection probability with a signal-to-noise ratio $S/N > 7$ is 53 mJy ms. To investigate how the completeness threshold would affect the modelling by q -Gaussians, we also perform a parallel comparative analysis of the complete subsample (i.e., those bursts with $F > 53$ mJy ms). We find that the mean values of q for energy, peak flux, duration, and waiting time are 2.43 ± 0.03 , 2.41 ± 0.02 , 1.38 ± 0.03 , and 2.56 ± 0.02 , respectively. Comparing these inferred q values with those obtained from the whole FAST sample (see line 2 in Table 2), it is clear that the completeness threshold in the energy distribution only has a minimal influence on our results.

2.2. Statistical properties of high-energy bursts

Using four small 25–32-m class radio telescopes (including the 25-m telescope in Stockert, Germany (St); the 25-m

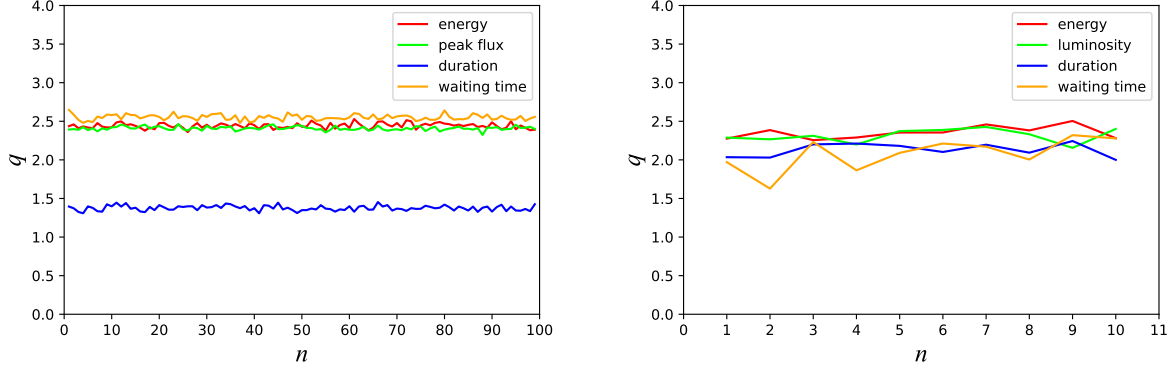


Figure 2. The best-fitting q values in the q -Gaussian distribution as a function of the temporal interval scale n for the samples of FAST (left panel) and high-energy bursts (right panel). The colors for different observed physical qualities (including energy, peak flux/luminosity, duration, and waiting time) are according to the legends.

Table 2. The average q values in the q -Gaussian distribution for FRB 20121102, FRB 20201124A, and glitches of PSR B1737–30

FRB name	Instrument	Energy range (erg)	Number	q -energy	q -flux	q -duration	q -waiting time	Refs.
20121102	FAST	4×10^{36} – 8×10^{39}	1652	2.51 ± 0.03	2.50 ± 0.03	1.42 ± 0.04	–	1
20201124A	FAST	1×10^{36} – 3×10^{39}	2744	2.44 ± 0.03	2.40 ± 0.02	1.37 ± 0.03	2.55 ± 0.03	2
20201124A	St, O8, Tr, Wb	2×10^{38} – 2×10^{40}	46	2.35 ± 0.07	2.31 ± 0.08	2.13 ± 0.08	2.07 ± 0.20	2
PSR name	Observatory	Glitch size range (μ Hz)	Number	q -glitch size			q -waiting time	Refs.
B1737–30	JBO	10^{-3} –4.4	37	2.38 ± 0.04			1.80 ± 0.18	2

NOTE—The second column of Table 2 is the instrument (observatory) for observing repeating FRBs (glitches of PSR B1737–30). The third column is the energy range (glitch size range) of repeating bursts of FRBs (glitches of PSR B1737–30). The fourth column represents the number of the corresponding sample. Columns 5–8 correspond to the average q values for different observed physical qualities (including energy/glitch size, flux, duration, and waiting time). The last column is the reference list: (1) Wei et al. (2021); (2) This work.

dish in Onsala, Sweden (O8); the 32-m dish in Toruń, Poland (Tr); and the 25-m dish in Westerbork, The Netherlands (Wb)), Kirsten et al. (2024) detected 46 high-energy bursts from FRB 20201124A. They concluded that the highest-energy bursts ($E > 3 \times 10^{39}$ erg) occur much more frequently than one would expect based on the energy distribution of lower-energy bursts observed by FAST. The hyperactive source FRB 20201124A provides a good opportunity to probe the high-energy distribution and to compare with low-energy bursts. Here we investigate whether the highest-energy bursts originate from a separate emission mechanism by comparing the scale-invariant properties of low- and high-energy bursts.

Due to the limited number of data points, the cumulative distribution function (CDF) is often used instead of PDF to avoid the arbitrariness caused by binning. We thus try to fit the CDF of fluctuations for high-energy bursts using the CDF of q -Gaussian, i.e.,

$$F(x_n) = \int_{-\infty}^{x_n} f(x_n) dx, \quad (5)$$

where $f(x_n)$ is the q -Gaussian function (Equation (3)). Similarly, with a fixed n , we obtain the best-fitting parameters (α , β , and q) by minimizing the χ^2 statistics,

$$\chi^2 = \sum_i \frac{[N_{\text{cum}}(< x_{n,i}) - F(x_{n,i})]^2}{\sigma_{\text{cum},i}^2}, \quad (6)$$

where $\sigma_{\text{cum},i} = \sqrt{N_{\text{cum}}(< x_{n,i})}$ denotes the uncertainty of the data point, with $N_{\text{cum}}(< x_{n,i})$ being the cumulative number of the fluctuations (Wei 2023).

Figure 3 shows some examples of the fits for the high-energy burst sample. In this plot, we display the CDFs of fluctuations of energy (upper-left panel), luminosity (upper-right panel), duration (lower-left panel), and waiting time (lower-right panel) for $n = 1$ (red dots), $n = 5$ (green dots), and $n = 10$ (blue dots). The best fitting q -values and the corresponding χ_{red}^2 values for $n = 1, 5, 10$ are presented in Table 1. From Figure 3 and the χ_{red}^2 values, we find that the CDFs of fluctuations of energy, luminosity, duration, and waiting time can be well fitted by the CDF of q -Gaussian function

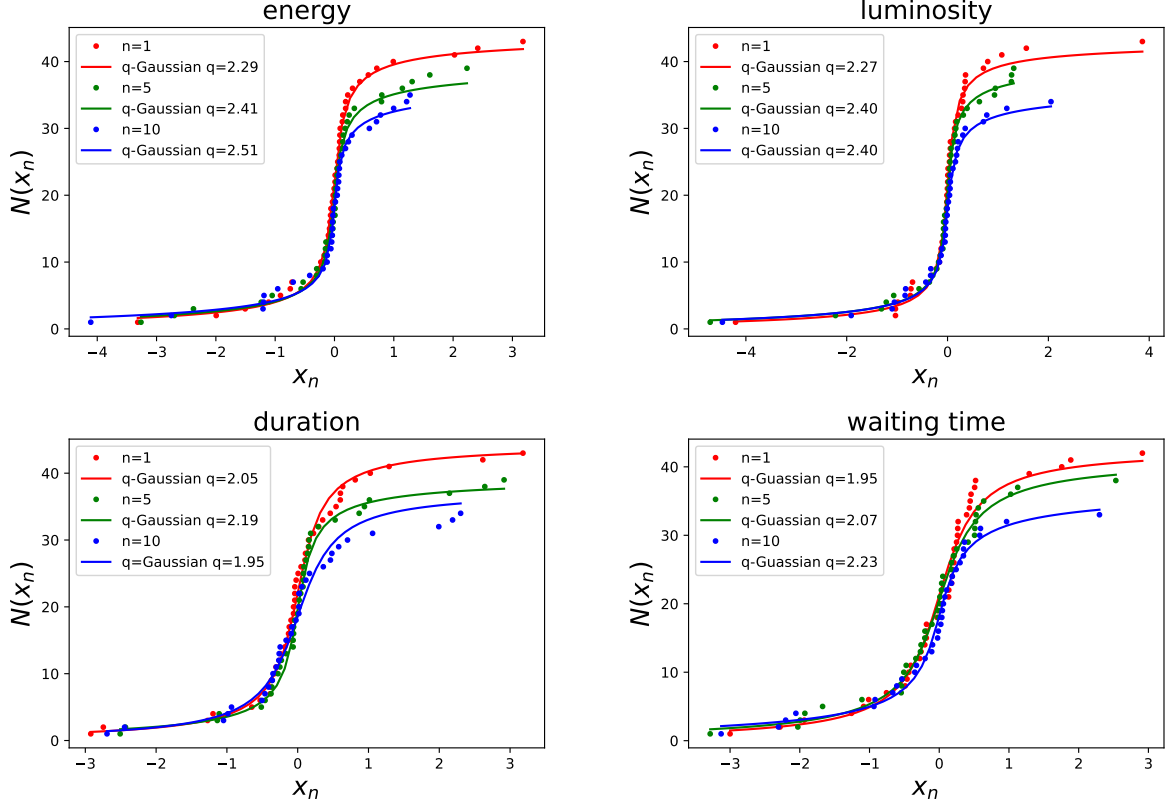


Figure 3. Statistical results of FRB 20201124A for the high-energy burst sample. *Upper-left panel:* The CDFs of energy fluctuations $X_n = S_{i+n} - S_i$ for different temporal interval scales $n = 1$ (red dots), $n = 5$ (green dots), and $n = 10$ (blue dots). X_n is rescaled by the standard deviation of X_n , i.e. $x_n = X_n/\sigma_{X_n}$. The data are fitted by the CDF of q -Gaussian function (solid curves). *The other three panels:* The same data process and the fitting to the CDF of q -Gaussian function, except now for the CDFs of fluctuations of luminosity (upper-right panel), duration (lower-left panel), and waiting time (lower-right panel).

(see solid curves). Moreover, we plot the best-fitting q values as a function of the temporal interval scale n in the range $1 \leq n \leq 10$, and find that the q values also keep approximately steady (see the right panel of Figure 2). The average q values of energy, luminosity, duration, and waiting time for the data of high-energy bursts are 2.35 ± 0.07 , 2.31 ± 0.08 , 2.13 ± 0.08 , and 2.07 ± 0.20 , respectively. As shown in Table 2, the q values of energy and luminosity (peak flux) of high-energy bursts are consistent with those of FAST observations of low-energy bursts within 1σ confidence level, but the q values of duration and waiting time between low- and high-energy bursts are significantly different.

One possible explanation for the different q values of duration and waiting time for low- and high-energy bursts of FRB 20201124A is that burst duration is subject to instrumental effects, thereby affecting the estimate of the waiting time. It is well known that the observed burst duration would be broadened by instrumental effects (Cordes & McLaughlin 2003). The instrumental burst broadening includes the intrachannel dispersion smearing and the sampling timescale. The smearing is due to intrachannel dispersion. The time resolution should not be better than the sampling timescale,

which broadens the burst. Therefore, different instruments may correspond to different broadening components. However, since we are interested in the statistical distributions of the differences of durations and waiting times at different time intervals, burst broadening induced by instrumental effects can be approximately deducted from subtracting two observed durations (or two waiting times). Thus, we conclude that the different q values for low- and high-energy bursts is likely not an instrumental effect. Rather, it more likely hints a differing emission mechanism or emission site between low- and high-energy bursts, although they originate from the same progenitor source.

3. SCALE INVARIANCE IN GLITCHING PULSARS

Remarkably, both a glitch and an antiglitch accompanied by FRB-like bursts from SGR J1935+2154 were recently reported. The temporal coincidences between the glitch/antiglitch and FRB-like bursts imply some physical connection between them (Ge et al. 2022; Younes et al. 2023). The statistical distributions of glitch sizes ($\Delta\nu$) and times between successive glitches (waiting times) for some individual pulsars are power-law forms (Morley & Garcia-

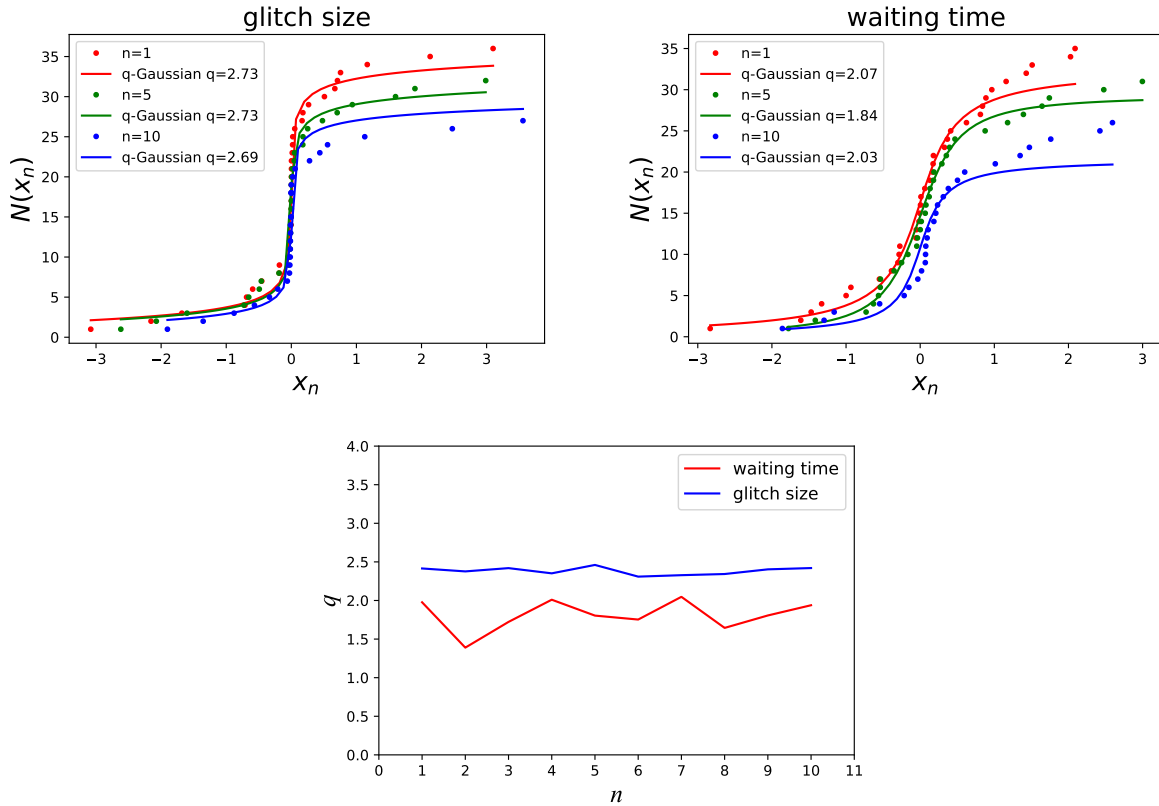


Figure 4. Statistical results of glitches of PSR B1737–30. *Upper-left panel:* The CDFs of glitch size fluctuations $X_n = S_{i+n} - S_i$ for different temporal interval scales $n = 1$ (red dots), $n = 5$ (green dots), and $n = 10$ (blue dots). X_n is rescaled by the standard deviation of X_n , i.e. $x_n = X_n / \sigma_{X_n}$. The data are fitted by the CDF of q -Gaussian function (solid curves). *Upper-right panel:* The same data process and the fitting to the CDF of q -Gaussian function, except now for the CDFs of waiting-time fluctuations. *Lower panel*

: The best-fitting q values in the q -Gaussian distribution as a function of n .

Pelayo 1993; Melatos et al. 2008; Carlin & Melatos 2021). Power-law distributions of energy and waiting time are also found in some repeating FRBs (Wang & Yu 2017; Katz 2018; Gourdjji et al. 2019; Cheng et al. 2020; Cruces et al. 2021; Li et al. 2021b; Zhang et al. 2021; Hewitt et al. 2022; Jahns et al. 2023; Wang et al. 2023). Inspired by the associations between the glitch/antiglitch and FRB-like bursts of SGR J1935+2154 and the statistical similarities between pulsar glitches and repeating FRBs, here we investigate whether pulsar glitches have a similar scale-invariant behavior.

To date, there are only eight pulsars with more than 10 detected glitches (Fuentes et al. 2019). PSR B1737–30 has been observed regularly by the Jodrell Bank Observatory (JBO), and 37 glitches have been detected over ~ 35 years. PSR B1737–30 has the largest number of glitch events among the glitching pulsars exhibiting power-law size distributions. Consequently, the statistical results for PSR B1737–30 are much more significant than other pulsars. Glitch epochs and sizes for the pulsars are available in the JBO online catalogue

(Espinoza et al. 2011)². Due to the relatively small sample of glitches, we also focus on the CDFs of fluctuations of glitch size and waiting time at different scale intervals n . For a fixed n , we use the CDF of q -Gaussian (Equation (5)) to fit the CDFs of fluctuations, and derive the best-fitting q value. Then we vary n and obtain the q values as a function of n .

For the detected glitches in PSR B1737–30, the CDFs of fluctuations of glitch size and waiting time are presented in the left and middle panels of Figure 4, respectively. The best-fitting q values and the corresponding χ^2_{red} values for $n = 1, 5, 10$ are listed in Table 1. It is clear that the q -Gaussian function fits the data points very well. To better highlight the scale-invariant property in PSR B1737–30’ glitches, the best-fitting q values as a function of n for glitch size and waiting time are plotted in the right panel of Figure 4. Again, we find that the q values are nearly constant and independent of n . We also list the average q values from $n = 1$ to 10 for glitch size ($\bar{q} = 2.38 \pm 0.04$) and waiting time ($\bar{q} = 1.80 \pm 0.18$) in Table 2. Interestingly, the average q values of glitch size (en-

² <http://www.jb.man.ac.uk/pulsar/glitches.html>

ergy) and waiting time are well consistent with those of FRB 20201124A’s high-energy bursts, which indicate that there may be an underlying physical connection between pulsar glitches and FRB 20201124A’s high-energy bursts.

4. SUMMARY AND DISCUSSION

SOC dynamics can be effectively identified and diagnosed by analyzing the avalanche size fluctuations (Caruso et al. 2007). When criticality appears, the PDFs for the avalanche size fluctuations at different times have fat tails with a q -Gaussian form. Such a q -Gaussian behavior is independent of the time interval adopted, and it is found so when considering energy fluctuations between real earthquakes (Caruso et al. 2007). That is, the q values in q -Gaussian distributions are nearly invariant for different temporal interval scales, implying a scale-invariant structure in earthquakes (see also Wang et al. 2015). Analogous scale-invariant characteristics have also been discovered in some astronomical phenomena, such as SGRs (Chang et al. 2017; Wei et al. 2021; Sang & Lin 2022), the repeating FRB 20121102 (Lin & Sang 2020; Wei et al. 2021), GRB X-ray flares (Wei 2023) and precursors (Li & Yang 2023), and gamma-ray flares of the Sun and the blazar 3C 454.3 (Peng et al. 2023). Given the temporal coincidences between the glitch/antiglitch and FRB-like bursts from the Galactic magnetar SGR J1935+2154 (Ge et al. 2022; Younes et al. 2023), here we examined their possible physical connection by comparing the scale-invariant similarities between repeating FRBs and glitching pulsars.

For repeating FRBs, we focused on the statistical properties of the hyperactive repeating source FRB 20201124A using two samples from different observations. The first sample contains 2744 bursts from the FAST observation, and the second one consists of 46 high-energy bursts from the observations of four small 25–32-m class radio telescopes. Note that except for FRB 20121102, it is unclear whether other repeating FRBs share the same scale-invariant property. With the FAST data, we confirmed that the PDFs of fluctuations of energy, peak flux, duration, and waiting time can be well fitted by a q -Gaussian function, and the q values keep nearly steady for different time scales. Moreover, we found that the average q values of energy, peak flux, and duration for the FAST data of FRB 20201124A are very close to those of FRB 20121102 (Wei et al. 2021), which indicate that there is a common scale-invariant feature in repeating FRBs. With

the high-energy burst sample, similar scale-invariant results were obtained, but the average q values of duration and waiting time of high-energy bursts are significantly different from those of FAST observations of low-energy bursts. This implies that low- and high-energy bursts may originate from different emission mechanisms or emission regions at the progenitor source. Wang et al. (2015) also found that different faulting styles correspond to different q values in earthquakes.

For glitching pulsars, we investigated the statistical properties of 37 known glitches from PSR B1737–30. We showed that the distributions of fluctuations of glitch size and waiting time also exhibit a q -Gaussian form, with constant q values independent of the adopted time scale. This scale-invariant property is very similar to those of repeating FRBs, and both the two astronomical phenomena can be attributed to a SOC process. Interestingly, the average q values of glitch size (energy) and waiting time align consistently with those of FRB 20201124A’s high-energy bursts, which suggest that there may be an underlying physical association between pulsar glitches and FRB 20201124A’s high-energy bursts.

In summary, our findings support the argument that both repeating FRBs and pulsar glitches can be explained within a dissipative SOC mechanism with long-range interactions. In the future, much more glitches and FRB-like bursts from the magnetars will be detected. The physical connection between glitches and FRB-like bursts can be further investigated.

1 We are grateful to the anonymous referee for construc-
 2 tive comments that helped improve our work. This
 3 work is partially supported by the National SKA Pro-
 4 gram of China (2022SKA0130100), the National Natu-
 5 ral Science Foundation of China (grant Nos. 12373053,
 6 12321003, and 12041306), the Key Research Program of
 7 Frontier Sciences (grant No. ZDBS-LY-7014) of Chinese
 8 Academy of Sciences, International Partnership Program
 9 of Chinese Academy of Sciences for Grand Challenges
 10 (114332KYSB20210018), the CAS Project for Young Scien-
 11 tists in Basic Research (grant No. YSBR-063), the CAS Or-
 12 ganizational Scientific Research Platform for National Major
 13 Scientific and Technological Infrastructure: Cosmic Tran-
 14 sients with FAST, and the Natural Science Foundation of
 15 Jiangsu Province (grant No. BK20221562).

REFERENCES

- Antonopoulou, D., Haskell, B., & Espinoza, C. M. 2022, Reports on Progress in Physics, 85, 126901, doi: [10.1088/1361-6633/ac9ced](https://doi.org/10.1088/1361-6633/ac9ced)
- Aschwanden, M. J. 2011, Self-Organized Criticality in Astrophysics
- . 2012, A&A, 539, A2, doi: [10.1051/0004-6361/201118237](https://doi.org/10.1051/0004-6361/201118237)
- . 2014, ApJ, 782, 54, doi: [10.1088/0004-637X/782/1/54](https://doi.org/10.1088/0004-637X/782/1/54)
- . 2015, ApJ, 814, 19, doi: [10.1088/0004-637X/814/1/19](https://doi.org/10.1088/0004-637X/814/1/19)
- Aschwanden, M. J., Crosby, N. B., Dimitropoulou, M., et al. 2016, SSRv, 198, 47, doi: [10.1007/s11214-014-0054-6](https://doi.org/10.1007/s11214-014-0054-6)

- Bak, P., Tang, C., & Wiesenfeld, K. 1987, *Physical Review Letters*, 59, 381, doi: [10.1103/PhysRevLett.59.381](https://doi.org/10.1103/PhysRevLett.59.381)
- Bochenek, C. D., Ravi, V., Belov, K. V., et al. 2020, *Nature*, 587, 59, doi: [10.1038/s41586-020-2872-x](https://doi.org/10.1038/s41586-020-2872-x)
- Carlin, J. B., & Melatos, A. 2021, *ApJ*, 917, 1, doi: [10.3847/1538-4357/ac06a2](https://doi.org/10.3847/1538-4357/ac06a2)
- Caruso, F., Pluchino, A., Latora, V., Vinciguerra, S., & Rapisarda, A. 2007, *PhRvE*, 75, 055101, doi: [10.1103/PhysRevE.75.055101](https://doi.org/10.1103/PhysRevE.75.055101)
- Chang, Z., Lin, H.-N., Sang, Y., & Wang, P. 2017, *Chinese Physics C*, 41, 065104, doi: [10.1088/1674-1137/41/6/065104](https://doi.org/10.1088/1674-1137/41/6/065104)
- Cheng, Y., Zhang, G. Q., & Wang, F. Y. 2020, *MNRAS*, 491, 1498, doi: [10.1093/mnras/stz3085](https://doi.org/10.1093/mnras/stz3085)
- CHIME/FRB Collaboration, Amiri, M., Andersen, B. C., et al. 2020a, *Nature*, 582, 351, doi: [10.1038/s41586-020-2398-2](https://doi.org/10.1038/s41586-020-2398-2)
- CHIME/FRB Collaboration, Andersen, B. C., Bandura, K. M., et al. 2020b, *Nature*, 587, 54, doi: [10.1038/s41586-020-2863-y](https://doi.org/10.1038/s41586-020-2863-y)
- Cordes, J. M., & McLaughlin, M. A. 2003, *ApJ*, 596, 1142, doi: [10.1086/378231](https://doi.org/10.1086/378231)
- Cruces, M., Spitler, L. G., Scholz, P., et al. 2021, *MNRAS*, 500, 448, doi: [10.1093/mnras/staa3223](https://doi.org/10.1093/mnras/staa3223)
- Espinoza, C. M., Lyne, A. G., Stappers, B. W., & Kramer, M. 2011, *Monthly Notices of the Royal Astronomical Society*, 414, 1679, doi: [10.1111/j.1365-2966.2011.18503.x](https://doi.org/10.1111/j.1365-2966.2011.18503.x)
- Fong, W.-f., Dong, Y., Leja, J., et al. 2021, *ApJL*, 919, L23, doi: [10.3847/2041-8213/ac242b](https://doi.org/10.3847/2041-8213/ac242b)
- Foreman-Mackey, D., Hogg, D. W., Lang, D., & Goodman, J. 2013, *PASP*, 125, 306, doi: [10.1086/670067](https://doi.org/10.1086/670067)
- Freedman, D., & Diaconis, P. 1981, *Probability Theory and Related Fields*, 57, 453, doi: <https://doi.org/10.1007/BF01025868>
- Fuentes, J. R., Espinoza, C. M., & Reisenegger, A. 2019, *A&A*, 630, A115, doi: [10.1051/0004-6361/201935939](https://doi.org/10.1051/0004-6361/201935939)
- Ge, M., Yang, Y.-P., Lu, F., et al. 2022, *arXiv e-prints*, arXiv:2211.03246, doi: [10.48550/arXiv.2211.03246](https://doi.org/10.48550/arXiv.2211.03246)
- Good, D., & Chime/Frb Collaboration. 2020, *The Astronomer's Telegram*, 14074, 1
- Gourdji, K., Michilli, D., Spitler, L. G., et al. 2019, *ApJL*, 877, L19, doi: [10.3847/2041-8213/ab1f8a](https://doi.org/10.3847/2041-8213/ab1f8a)
- Haskell, B., & Melatos, A. 2015, *International Journal of Modern Physics D*, 24, 1530008, doi: [10.1142/S0218271815300086](https://doi.org/10.1142/S0218271815300086)
- Hewitt, D. M., Snelders, M. P., Hessels, J. W. T., et al. 2022, *MNRAS*, 515, 3577, doi: [10.1093/mnras/stac1960](https://doi.org/10.1093/mnras/stac1960)
- Huang, Y. F., & Geng, J. J. 2014, *ApJL*, 782, L20, doi: [10.1088/2041-8205/782/2/L20](https://doi.org/10.1088/2041-8205/782/2/L20)
- Jahns, J. N., Spitler, L. G., Nimmo, K., et al. 2023, *MNRAS*, 519, 666, doi: [10.1093/mnras/stac3446](https://doi.org/10.1093/mnras/stac3446)
- Katz, J. I. 1986, *Journal of Geophysical Research*, 91, 10412, doi: [10.1029/jb091ib10p10412](https://doi.org/10.1029/jb091ib10p10412)
- Katz, J. I. 2018, *MNRAS*, 476, 1849, doi: [10.1093/mnras/sty366](https://doi.org/10.1093/mnras/sty366)
- Kirsten, F., Ould-Boukattine, O. S., Herrmann, W., et al. 2024, *Nature Astronomy*, doi: [10.1038/s41550-023-02153-z](https://doi.org/10.1038/s41550-023-02153-z)
- Lanman, A. E., Andersen, B. C., Chawla, P., et al. 2022, *ApJ*, 927, 59, doi: [10.3847/1538-4357/ac4bc7](https://doi.org/10.3847/1538-4357/ac4bc7)
- Li, C. K., Lin, L., Xiong, S. L., et al. 2021a, *Nature Astronomy*, 5, 378, doi: [10.1038/s41550-021-01302-6](https://doi.org/10.1038/s41550-021-01302-6)
- Li, D., Wang, P., Zhu, W. W., et al. 2021b, *Nature*, 598, 267, doi: [10.1038/s41586-021-03878-5](https://doi.org/10.1038/s41586-021-03878-5)
- Li, X.-J., & Yang, Y.-P. 2023, *ApJL*, 955, L34, doi: [10.3847/2041-8213/acf12c](https://doi.org/10.3847/2041-8213/acf12c)
- Lin, H. N., & Sang, Y. 2020, *Monthly Notices of the Royal Astronomical Society*, 491, 2156, doi: [10.1093/mnras/stz3149](https://doi.org/10.1093/mnras/stz3149)
- Lorimer, D. R., Bailes, M., McLaughlin, M. A., Narkevic, D. J., & Crawford, F. 2007, *Science*, 318, 777, doi: [10.1126/science.1147532](https://doi.org/10.1126/science.1147532)
- Mastrano, A., Suvorov, A. G., & Melatos, A. 2015, *MNRAS*, 453, 522, doi: [10.1093/mnras/stv1658](https://doi.org/10.1093/mnras/stv1658)
- Melatos, A., Peralta, C., & Wyithe, J. S. B. 2008, *ApJ*, 672, 1103, doi: [10.1086/523349](https://doi.org/10.1086/523349)
- Mereghetti, S., Savchenko, V., Ferrigno, C., et al. 2020, *ApJL*, 898, L29, doi: [10.3847/2041-8213/aba2cf](https://doi.org/10.3847/2041-8213/aba2cf)
- Morley, P. D., & Garcia-Pelayo, R. 1993, *EPL (Europhysics Letters)*, 23, 185, doi: [10.1209/0295-5075/23/3/005](https://doi.org/10.1209/0295-5075/23/3/005)
- Peng, F.-K., Wei, J.-J., & Wang, H.-Q. 2023, *ApJ*, 959, 109, doi: [10.3847/1538-4357/acfc62](https://doi.org/10.3847/1538-4357/acfc62)
- Petroff, E., Hessels, J. W. T., & Lorimer, D. R. 2022, *A&A Rv*, 30, 2, doi: [10.1007/s00159-022-00139-w](https://doi.org/10.1007/s00159-022-00139-w)
- Piro, L., Bruni, G., Troja, E., et al. 2021, *A&A*, 656, L15, doi: [10.1051/0004-6361/202141903](https://doi.org/10.1051/0004-6361/202141903)
- Rajwade, K. M., Mickaliger, M. B., Stappers, B. W., et al. 2020, *MNRAS*, 495, 3551, doi: [10.1093/mnras/staa1237](https://doi.org/10.1093/mnras/staa1237)
- Ravi, V., Law, C. J., Li, D., et al. 2022, *MNRAS*, 513, 982, doi: [10.1093/mnras/stac465](https://doi.org/10.1093/mnras/stac465)
- Ridnaia, A., Svinikin, D., Frederiks, D., et al. 2021, *Nature Astronomy*, 5, 372, doi: [10.1038/s41550-020-01265-0](https://doi.org/10.1038/s41550-020-01265-0)
- Sang, Y., & Lin, H.-N. 2022, *MNRAS*, 510, 1801, doi: [10.1093/mnras/stab3600](https://doi.org/10.1093/mnras/stab3600)
- Spitler, L. G., Scholz, P., Hessels, J. W. T., et al. 2016, *Nature*, 531, 202, doi: [10.1038/nature17168](https://doi.org/10.1038/nature17168)
- Tavani, M., Casentini, C., Ursi, A., et al. 2021, *Nature Astronomy*, 5, 401, doi: [10.1038/s41550-020-01276-x](https://doi.org/10.1038/s41550-020-01276-x)
- Thompson, C., Duncan, R. C., Woods, P. M., et al. 2000, *ApJ*, 543, 340, doi: [10.1086/317072](https://doi.org/10.1086/317072)
- Tsallis, C. 1988, *Journal of Statistical Physics*, 52, 479, doi: [10.1007/BF01016429](https://doi.org/10.1007/BF01016429)
- Tsallis, C., Mendes, R., & Plastino, A. R. 1998, *Physica A Statistical Mechanics and its Applications*, 261, 534, doi: [10.1016/S0378-4371\(98\)00437-3](https://doi.org/10.1016/S0378-4371(98)00437-3)
- Wang, F. Y., Wu, Q., & Dai, Z. G. 2023, *ApJL*, 949, L33, doi: [10.3847/2041-8213/acd5d2](https://doi.org/10.3847/2041-8213/acd5d2)
- Wang, F. Y., & Yu, H. 2017, *JCAP*, 2017, 023, doi: [10.1088/1475-7516/2017/03/023](https://doi.org/10.1088/1475-7516/2017/03/023)

- Wang, P., Chang, Z., Wang, H., & Lu, H. 2015, *European Physical Journal B*, 88, 206, doi: [10.1140/epjb/e2015-60441-6](https://doi.org/10.1140/epjb/e2015-60441-6)
- Wei, J.-J. 2023, *Physical Review Research*, 5, 013019, doi: [10.1103/PhysRevResearch.5.013019](https://doi.org/10.1103/PhysRevResearch.5.013019)
- Wei, J.-J., Wu, X.-F., Dai, Z.-G., et al. 2021, *The Astrophysical Journal*, 920, 153, doi: [10.3847/1538-4357/ac2604](https://doi.org/10.3847/1538-4357/ac2604)
- Wu, Q., Zhao, Z.-Y., & Wang, F.-Y. 2023, *MNRAS*, 523, 2732, doi: [10.1093/mnras/stad1585](https://doi.org/10.1093/mnras/stad1585)
- Xiao, D., Wang, F., & Dai, Z. 2021, *Science China Physics, Mechanics, and Astronomy*, 64, 249501, doi: [10.1007/s11433-020-1661-7](https://doi.org/10.1007/s11433-020-1661-7)
- Xu, H., Niu, J. R., Chen, P., et al. 2022, *Nature*, 609, 685, doi: [10.1038/s41586-022-05071-8](https://doi.org/10.1038/s41586-022-05071-8)
- Younes, G., Baring, M. G., Harding, A. K., et al. 2023, *Nature Astronomy*, 7, 339, doi: [10.1038/s41550-022-01865-y](https://doi.org/10.1038/s41550-022-01865-y)
- Zhang, B. 2020, *Nature*, 587, 45, doi: [10.1038/s41586-020-2828-1](https://doi.org/10.1038/s41586-020-2828-1)
- . 2023, *Reviews of Modern Physics*, 95, 035005, doi: [10.1103/RevModPhys.95.035005](https://doi.org/10.1103/RevModPhys.95.035005)
- Zhang, G. Q., Wang, P., Wu, Q., et al. 2021, *ApJL*, 920, L23, doi: [10.3847/2041-8213/ac2a3b](https://doi.org/10.3847/2041-8213/ac2a3b)
- Zhang, Y.-K., Wang, P., Feng, Y., et al. 2022, *Research in Astronomy and Astrophysics*, 22, 124002, doi: [10.1088/1674-4527/ac98f7](https://doi.org/10.1088/1674-4527/ac98f7)
- Zhou, D. J., Han, J. L., Zhang, B., et al. 2022, *Research in Astronomy and Astrophysics*, 22, 124001, doi: [10.1088/1674-4527/ac98f8](https://doi.org/10.1088/1674-4527/ac98f8)